Micromagnetic analysis of remanence and coercivity of nanocrystalline Pr–Fe–B magnets

D. Suess
Institut für Angewandte und Technische Physik, Vienna University of Technology, Wiedner Hauptstr. 8-10, A-1040 Vienna, Austria

M. Dahlgren
Institut für Experimentalphysik, Vienna University of Technology, Wiedner Hauptstr. 8-10, A-1040 Vienna, Austria

T. Schrefl[a)]
Institut für Angewandte und Technische Physik, Vienna University of Technology, Wiedner Hauptstr. 8-10, A-1040 Vienna, Austria

R. Grössinger
Institut für Experimentalphysik, Vienna University of Technology, Wiedner Hauptstr. 8-10, A-1040 Vienna, Austria

J. Fidler
Institut für Angewandte und Technische Physik, Vienna University of Technology, Wiedner Hauptstr. 8-10, A-1040 Vienna, Austria

Nanocrystalline exchange coupled $Pr_{11.76}Fe_{82.36}B_{5.88}$ single-phase and $Pr_9Fe_{85}B_6$ two-phase magnets containing 20 vol % α-Fe were produced using mechanical alloying. Micromagnetic finite element simulations were used to analyze the temperature dependence of the magnetic properties. In the single-phase exchange-coupled magnet a significant enhancement of the remanence $J_r = 1.1$ T was achieved at room temperature. A further enhancement of the remanence was observed in two-phase α-Fe containing magnets reaching a remanence of $J_r = 1.23$ T. The corresponding values of the coercive field are $\mu_0 H_c = 0.81$ T and $\mu_0 H_c = 0.57$ T for the single-phase magnet and the two-phase magnet, respectively. Remanence enhancement becomes more effective with increasing temperature, compensating the decrease of the saturation polarization. In the two-phase magnet the remanence increases from $J_r = 1.12$ to $J_r = 1.23$ T as the temperature is increased from 200 to 300 K. Micromagnetic calculations clearly show that the increase of the exchange length with increasing temperature improves the effective coupling between the $Pr_2Fe_{14}B$ and the α-Fe phase. The decrease of the coercive field with increasing temperature has to be attributed to the temperature dependence of the anisotropy field. © *2000 American Institute of Physics.* [S0021-8979(00)41208-9]

I. INTRODUCTION

In the past decade a lot of attention was paid to a new kind of family of magnets (nanocrystalline and nanocomposite hard magnetic materials) based on rare-earth magnets where alignment is not necessary and the expensive rare-earth part is reduced.[1,2] These new kinds of materials are mainly characterized by an increase over the expected remanence of 50% from the saturation magnetization that is expected for an ensemble of noninteracting isotropic magnetic uniaxial grains.[3] These materials can be magnetized in relatively low fields and in any direction, because they are crystallographically isotropic. The nanocrystalline magnets with enhanced remanence can be divided into single-phase magnets and two-phase magnets composed of hard and soft magnetic phases which are also known as spring magnets.[4]

Nanocomposite α-Fe/$Nd_2Fe_{14}B$ has been produced by the melt spun technique[5] and mechanical alloying.[6] Significantly better combinations of the coercive field and the maximum energy product were reported for two-phase $Pr_2Fe_{14}B$ based magnets,[7] resulting from the higher anisotropy field of the $Pr_2Fe_{14}B$ phase as compared to $Nd_2Fe_{14}B$. As $Pr_2Fe_{14}B$ shows no spin reorientation, the temperature dependence of remanence and the coercive field of nanocomposite magnets can be studied for the α-Fe/$Pr_2Fe_{14}B$ system. Goll and co-workers[8] reported an improved thermal stability of the remanence with increasing α-Fe content.

This work combines the experimental measurements with micromagnetic calculations in order to analyze the temperature dependence of the magnetic properties of mechanically alloyed $Pr_2Fe_{14}B$ based nanocrystalline magnets. The mechanically alloyed samples have a much higher sample mass compared to melt spun flakes. The higher mass gives a much better signal-to-noise ratio which also enables measurements of the anisotropy field at low temperatures. For the mechanically alloyed Pr–Fe–B samples it is therefore possible to test existing predictions and models by using all necessary parameters such as grain size, anisotropy field, remanence, saturation polarization, and coercivity. Section II article of the describes the experimental detail, Sec. III introduces the simulation model, and Sec. IV compares the experimental findings with the numerical results.

[a)]Electronic mail: schrefl@email.tuwien.ac.at

II. EXPERIMENT

Nanocrystalline $Pr_{11.76}Fe_{82.36}B_{5.88}$ single-phase and $Pr_9Fe_{85}B_6$ two-phase magnets were produced using mechanical alloying. In order to receive mechanical alloyed magnets in the nanocrystalline state, the powder was compacted during a hot pressing procedure. The optimum hot pressing procedure was obtained by hot pressing the samples at 600 °C by heating without pressure under 2 min and under a pressure of 300 MPa under 2 min. For the samples produced, no induced anisotropy was found by measuring the hysteresis in the radial as well as in the *z* axis of the cylinder formed magnet. All the samples were magnetically characterized in a vibrating sample magnetometer operating in fields up to 8 T.

From x-ray diffraction using Cr $K\alpha_i$ radiation two crystallographic phases, i.e., the tetragonal $Pr_2Fe_{14}B$ phase and the body-centered-cubic (bcc) α-Fe phase, were detected in the low stoichiometric $Pr_9Fe_{85}B_6$ sample. The volume fraction of 20% α-Fe was derived from the measured saturation polarization of $J_s=1.75$ at $T=300$ K, assuming $J_s=2.15$ and $J_s=1.62$ for α-Fe and $Pr_2Fe_{14}B$, respectively.

The grain size distributions were determined by the convolute x-ray line-broadening analysis. The mean grain size of the stoichiometric Pr–Fe–B magnet was 24 nm, in the two-phase magnet the mean grain size of the $Pr_2Fe_{14}B$ grain and the α-Fe grains were 27 and 17 nm, respectively. The singular point detection technique was used to directly determine the anisotropy field of the isotropic samples. The nanocrystalline samples with an enhanced remanence at room temperature, $Pr_{11.76}Fe_{82.36}B_{5.88}$ and $Pr_9Fe_{85}B_6$, have a lower anisotropy field than an over stoichiometric $Pr_{18}Fe_{76}B_6$ magnet that is not remanence enhanced (see Table II). This reduction of the anisotropy field at room temperature is a strong indication of the magnetic exchange interactions between the grains. The actual direction of the final easy magnetization could be the energetic compromise of the surrounding nanocrystallites. This slightly tilted easy magnetization direction gives a natural reduction of the anisotropy field. If the average grain size is increased the influence of the exchange interaction would be weaker, since the exchange interactions between the grains would not influence the bulk part of the grains.

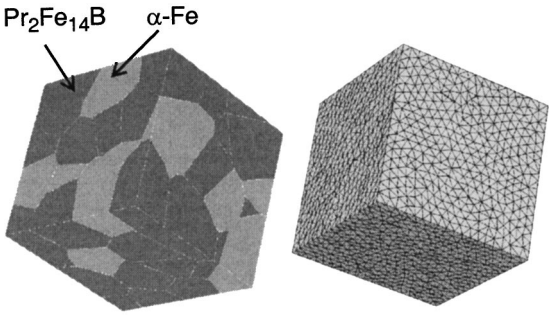

FIG. 1. Model of the nanocomposite magnet used for the simulation. The gray regions correspond to soft magnetic α-Fe grains, the black regions denote hard magnetic $Pr_2Fe_{14}B$ grains. The total number of grains is 64. The figure on the right hand side shows the triangulation of the grains into finite elements.

III. SIMULATION MODEL

The hysteresis properties were simulated using a micromagnetic finite element model. The demagnetization curve was calculated from the repeated minimization of the total Gibb's free energy for decreasing the external field. The initial state for this process was the fully saturated sample. A conjugate gradient method is applied to find the next local minimum of the energy. The magnetostatic field is calculated similar to standard finite element field calculation packages, using a magnetic vector potential and space transformations to treat the open boundary problem. Details of the algorithm are given in Refs. 9 and 10.

Figure 1 gives the finite element model of the two-phase $Pr_9Fe_{85}B_6$ magnet used for the calculation. The intrinsic magnetic properties were taken from the measurements. The total number of grains is 64. The mean grain size of both phases was assumed to be 24 nm. Owing to the limited number of grains in the model, it was not possible to assign different grain sizes to α-Fe and $Pr_2Fe_{14}B$ grains. The very same grain structure was used for the single-phase magnet, expect that the α-Fe grains were replaced by $Pr_2Fe_{14}B$ grains. Table I summarizes the intrinsic magnetic properties used for the calculations.

TABLE I. Comparison of the measured and calculated magnetic properties. H_a denotes the measured anisotropy field, H_c is the coercive field, and J_r is the remanence.

	$\mu_0 H_a$ (T)	H_c/H_a	$\mu_0 H_c$ (T)	J_r/J_s	J_r (T)
$Pr_{11.76}Fe_{82.36}B_{5.88}$, 200 K	11.4	0.15	1.65	0.63	1.07
Simulation	···	0.21	2.4	0.59	1.0
$Pr_{11.76}Fe_{82.36}B_{5.88}$, 300 K	8	0.10	0.81	0.68	1.1
Simulation	···	0.19	1.54	0.62	1.0
$Pr_9Fe_{85}B_6$, 200 K	11.3	0.092	1.05	0.63	1.12
Simulation	···	0.15	1.7	0.66	1.17
$Pr_9Fe_{85}B_6$, 300 K	7.4	0.08	0.57	0.7	1.23
Simulation	···	0.12	0.89	0.71	1.26

TABLE II. Intrinsic magnetic properties used for the calculations. The anisotropy constants K_1 and K_2, the saturation polarization J_s, and the exchange constant A.

	K_1 (kJ/m^3)	K_2 (kJ/m^3)	J_s (T)	A (pJ/m)
$Pr_2Fe_{14}B$, 200 K	7600	0	1.69	6.9
$Pr_2Fe_{14}B$, 300 K	5200	0	1.62	6.4
α-Fe, 200 K	51	11	2.15	25
α-Fe, 300 K	46	15	2.15	25

IV. RESULTS AND DISCUSSION

Table II compares the experimental results with the simulated values of the remanence and the coercive field. The numerical results for the remanence agree well with the experimental values. The calculated coercivities are over approximated due to the assumption of perfect grain boundaries. The experiments and the simulations show only a weak dependence of the ratio of coercivity and the anisotropy field as a function of temperature (Fig. 2). Thus, the decrease of the coercive field with increasing temperature has to be attributed to the temperature dependence of the anisotropy field.

The stoichiometric $Pr_{11.76}Fe_{82.36}B_{5.88}$ shows a ratio remanence to saturation polarization just below 0.7 at room temperature. This clearly indicates an intergrain exchange interaction. The ratio remanence to saturation polarization is decreasing at about 200 K down to 0.6. This decrease is an indication that the coupling between the grains are weakened resulting in a lower ratio. This was expected, since the exchange length is declining, resulting in a weaker exchange coupling at lower temperatures. The same behavior is also observed for the under stoichiometric $Pr_9Fe_{85}B_6$. The decrease of the exchange length, $l_k=(2A/H_aJ_s)^{0.5}$, is mainly due to the increase of the anisotropy field H_a at lower temperatures. As the temperature is decreased from 300 to 200 K, the exchange length decreases from 1.1 to 0.95 nm and from 1.15 to 0.95 nm for $Pr_{11.76}Fe_{82.36}B_{5.88}$ and $Pr_9Fe_{85}B_6$, respectively. The higher exchange length at room temperature improves the effective coupling between the grains. This effect compensates the decrease of the saturation polarization with increasing temperature. As a consequence, the remanence remains nearly constant as a function of temperature in the stoichiometric sample and increases with increasing temperature for the two- phase α-Fe containing magnet.

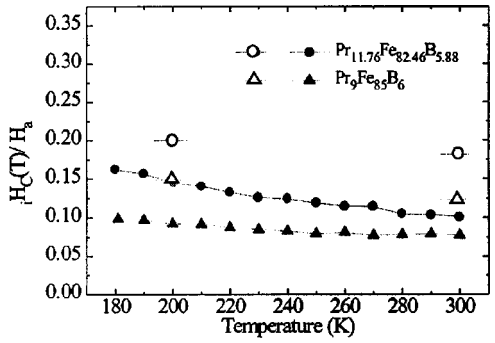

FIG. 2. Temperature dependence of the ratio coercivity to anisotropy. Closed symbols: mechanically alloyed Pr–Fe–B magnets, open symbols: micromagnetic simulation.

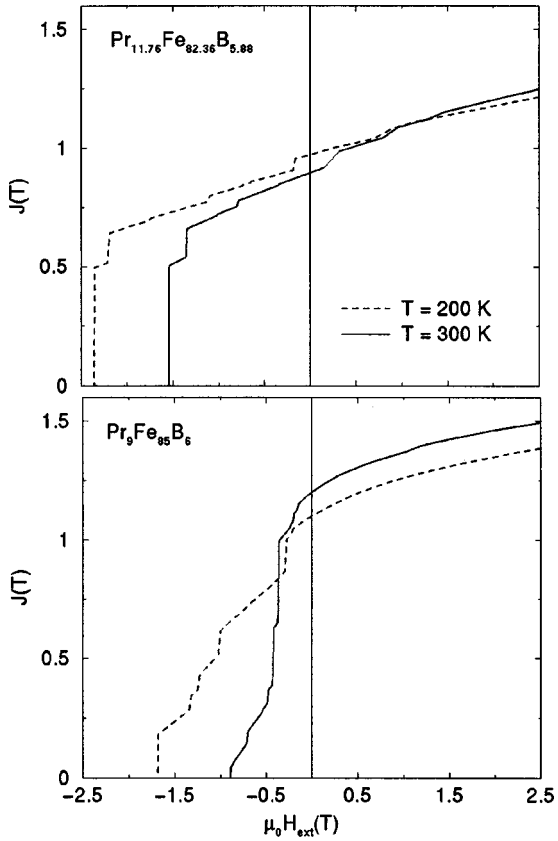

FIG. 3. Calculated demagnetization curves for the single-phase $Pr_{11.76}Fe_{82.36}B_{5.88}$ and the two-phase α-Fe/$Pr_2Fe_{14}B$ magnet at 200 and 300 K.

Figure 3 compares the calculated demagnetization curves for 200 and 300 K. The numerical results clearly demonstrate the temperature dependence of the magnetic properties. The coercivity decreases with increasing temperature in both $Pr_{11.76}Fe_{82.36}B_{5.88}$ and $Pr_9Fe_{85}B_6$. The temperature dependence of the remanence is less significant. The analysis of stable magnetization configurations for low opposing external fields shows that the magnetization remains more uniform at room temperature than at 200 K, owing to an improved exchange coupling of the grains.

[1] R. Coehoorn, D. B. de Mooij, J. P. W. B. Duchateau, and K. H. J. Bushow, J. Phys. C **8**, 669 (1988).
[2] A. M. Kadin, R. W. McCallum, G. M. Clemente, and J. E. Keem, in *Science and Technology of Rapidly Quenched Alloys*, edited by M. Tenhover, W. L. Johnson, and L. E. Tanner [Mater. Res. Soc. Symp. Proc. **80**, 385 (1987)].
[3] E. C. Stoner and E. P. Wohlfarth, Philos. Trans. R. Soc. London **240**, 599 (1948).
[4] E. F. Kneller, IEEE Trans. Magn. **27**, 3588 (1991).
[5] A. Manaf, R. A. Buckley, and H. A. Davies, J. Magn. Magn. Mater. **128**, 302 (1993).
[6] J. Wecker, K. Schnitzke, H. Cerva, and W. Grogger, Appl. Phys. Lett. **67**, 563 (1995).
[7] G. Mendoza-Suarez and H. A. Davies, J. Alloys Compd. **281**, 17 (1998).
[8] D. Goll, M. Seeger, and H. Kronmüller, J. Magn. Magn. Mater. **185**, 49 (1998).
[9] T. Schrefl, J. Fidler, and H. Kronmüller, Phys. Rev. B **49**, 6100 (1994).
[10] T. Schrefl, J. Fidler, and H. Kronmüller, J. Magn. Magn. Mater. **138**, 15 (1994).